Effects of Vehicle Speed in Structural Health Monitoring from Operational Conditions of Bridges

V. Jaksic
Dynamial Systems and Risk Laboratory, Department of Civil and Environmental Engineering, University College Cork, Ireland

A. O'Connor
Department of Civil, Structural and Environmental Engineering, Trinity College Dublin, Ireland

V. Pakrashi
Dynamial Systems and Risk Laboratory, Department of Civil and Environmental Engineering, University College Cork, Ireland

ABSTRACT: The effects of vehicle speed for Structural Health Monitoring (SHM) of bridges under operational conditions are studied in this paper. The moving vehicle is modelled as a single degree oscillator traversing a damaged beam at a constant speed. The bridge is modelled as simply supported Euler-Bernoulli beam with a breathing crack. The breathing crack is treated as a nonlinear system with bilinear stiffness characteristics related to the opening and closing of crack. The unevenness of the bridge deck is modelled using road classification according to ISO 8606:1995(E). The stochastic description of the unevenness of the road surface is used as an aid to monitor the health of the structure in its operational condition. Numerical simulations are conducted considering the effects of changing vehicle speed with regards to cumulant based statistical damage detection parameters. The detection and calibration of damage at different levels is based on an algorithm dependent on responses of the damaged beam due to passages of the load. Possibilities of damage detection and calibration under benchmarked and non-benchmarked cases are considered. Sensitivity of calibration values is studied. The findings of this paper are important for establishing the expectations from different vehicle speeds on a bridge for damage detection purposes using bridge-vehicle interaction where the bridge does not need to be closed for monitoring. The identification of bunching of these speed ranges provides guidelines for using the methodology developed in the paper.

1 INTRODUCTION

Structural Health Monitoring (SHM) addresses the continuous monitoring of a structure in terms of static and dynamic response, including the diagnoses of the onset of anomalous structural behavior (Moyo and Brownjohn, 2002). Non-destructive structural damage detection, in this regard, is becoming an important aspect of integrity assessment for aging, extreme-event affected or inaccessible structures (Kisa, 2004; Rucka and Wilde, 2006; Farrar and Worden, 2007; Pakrashi et al., 2009).

Presence of damage in a structure often only influences the change in local dynamic characteristics of the system observed. Therefore there is a need to establish the appropriate damage detection markers to capture such local dynamic changes. In this regard, employing bridge–vehicle interaction models for damage detection and SHM has gained considerable interest in recent times (Delgado and dos Santos, 1997; Pakrashi et al., 2010.

Bilello and Bergman (2004) have observed the response of smooth surface damaged Euler–Bernoulli beam traversed by a moving mass, where the damage was modelled through rotational springs. Bu et al.(2006) have proposed damage assessment approach from the dynamic response of a passing vehicle through a damage index. Poor Road Surface Roughness (RSR) was observed to be a bad detector for damage in their approach.

Pesterev and Bergman (1997) proposed a method for solving the problem of dynamic response of an elastic structure carrying a moving oscillator with arbitrarily varying speed. Majumdar and Manohar (2003) have proposed time domain damage descriptor to reflect the changes in bridge behavior due to damage. Law and Zhu (2005) have studied the effect of interaction between the structure, the road surface roughness and the vehicle.

Pakrashi et al. (2010) have performed experimental investigation of simply supported beam with moving load considering different level of damage. Local damage in beams have been modelled in a number of ways (Friswell and Penny, 2002). Narkis (1994) has proposed a method for calculation of natural frequencies of a cracked simply supported beam using an equivalent rotational spring.

Sundermeyer and Weaver (1994) have exploited the non-linear character of vibrating beam with a breathing crack. The effect of vehicle speed in combination with different grade of surface roughness, location and extent of damage on bridges has never been used

as an aid to damage detection. This paper investigates influence and sensitivity of vehicle speed on damage detection of beam-like structures through bridge vehicle interaction, taking into the account road quality.

Harris et al (2010) have proposed a method for characterisation of pavement roughness through the analysis of vehicle acceleration. Fryba (1999) has shown the effect of RSR on bridge response. Abdel-Rohman and Al-Duaij (1996) investigated the effects of unevenness in the bridge deck on the dynamic response of a single span bridge due to the moving loads.

O'Brien et al. (2006) have proposed a Bridge Roughness Index (BRI) which gives insight into the contribution that road roughness makes to dynamics of simply supported bridges. Da Silva (2004) has proposed a methodology to evaluate the dynamical effects, displacement and stress on highway bridge decks due to vehicle crossing on rough pavement surfaces.

Although there are many interesting numerical and statistical markers and methods available for damage detection (Sohn et al., 2001; Cacciola et al., 2003; Hadjileontiadis et al., 2005; Hadjileontiadis et al., 2007) surface roughness has always been treated for parameter studies, improved analysis or for establishing the bounds of efficiency of an algorithm.

Jaksic et al. (2011) have very recently investigated the potential of using surface roughness for detecting damage where a white noise excitation response of a single degree of freedom bilinear oscillator was investigated.

The white noise represented a broadband excitation, qualitatively similar to the interaction with surface roughness and the bilinearity attempted to capture a breathing crack. First and second order cumulants of the response of this system were observed to be appropriate markers for detecting changes in system stiffness.

In this paper a beam-vehicle interaction based damage detection from multiple point observations in the time domain using the interaction with realistic surface roughness testing the effects of range of the vehicle speed is presented. The damage has been modelled as a localized breathing crack and surface roughness has been defined by ISO 8606:1995 (1995).

The responses of the first mode of undamaged and damaged beam are observed (Poudel et al., 2005) since they are often easy to detect and are often a good approximation of the actual displacement. The vehicle speed in conjunction with preferable road quality for such detection process is investigated in this paper.

2 DAMAGED BRIGE-VEHICLE INTERACTION PROBLEM FORMULATION

The model of damaged bridge-vehicle interaction system is represented as a simply supported Euler–Bernoulli beam with a breathing crack traversed by a single degree of freedom (SDOF) oscillator presenting the vehicle. The schematic of the model considered is presented in Fig. 1. The symbols related to all equations are provided in Section 7 os this paper.

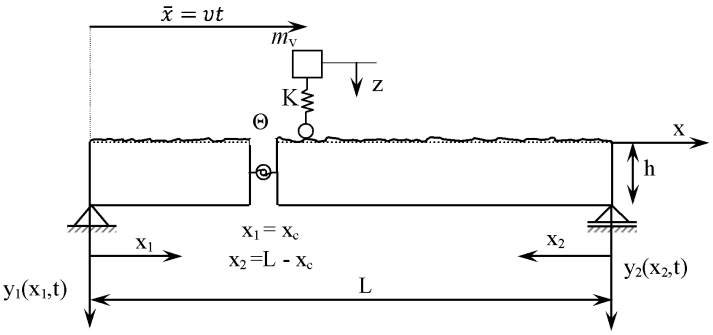

Figure 1. Simply supported beam with breathing crack modeled as two beams connected by torsional spring.

The vehicle is assumed to be moving on the surface without losing contact. The surface roughness is defined by ISO 8606:1995(E)26. The beam geometry and material characteristics are assumed constant. The crack can be modeled as a rotational spring15 when the crack is open. The equation of motion of the interaction between the beam and the SDOF oscillator is given by:

$$EI\frac{\partial^4 y_i(x,t)}{\partial x^4} + c\frac{\partial y_i(x,t)}{\partial t} + \rho A\frac{\partial^2 y_i(x,t)}{\partial t^2} = P\delta(x-\upsilon t); \quad i = 1,2 \tag{1}$$

The external force is defined as

$$P = m_v g + K\left[z - y_i(\upsilon t, t) - r(\upsilon t)\right] \quad i = 1,2 \tag{2}$$

$$K[z - y_i(\upsilon t,t) - r(\upsilon t)\,] \geq 0 \tag{3}$$

The solutions of the eigenvalue problem related to this system for the open and the closed crack stages provide the natural frequencies and mode shapes. When the crack is open, the system consists of two beams connected by torsional spring, where each continuous segment of the beam can be described by the Bernoulli-Euler partial differential equation of motion. The eigenvalue problem can then be solved through the method of separation of variables:

$$y_i(x,t) = \sum_{j=0}^{n} \phi_j^i(x) q_j(t); \quad i = 1, 2 \tag{4}$$

By separating temporal and spatial variables, the following differential equation system is obtained:

$$\phi_i^{iv}(x) - \frac{\omega_j^2 \rho A}{EI} \phi_j^i(x) = 0; \quad i = 1, 2; \quad j = 1 \, to \, n \tag{5}$$

$$\ddot{q}_j(t) + \omega_j^2 q_j(t) = 0; \quad j = 1 \, to \, n \tag{6}$$

For free vibrations of the beam, there is no external excitation and consequently there are no displacements or moments at the supports. Also, boundary conditions at the crack location x_c must satisfy continuity of displacement, bending moment and shear and the slope between the two beam segments can be related to the moment at this section. The solution of the spatial differential Eq. (5) satisfying all eight boundary conditions is:

$$0 < \bar{x} < x_c \quad \rightarrow \quad \phi = A_0(\sin a\bar{x} + \alpha \sinh a\bar{x}) \tag{7}$$

$$x_c < \bar{x} < L \quad \rightarrow \quad \phi = A_0\left(\frac{sin(ax_c)\,sin(a(L-\bar{x}))}{sin(a(L-x_c))} + \alpha \frac{sinh(ax_c)\,sinh(a(L-\bar{x}))}{sinh(a(L-x_c))}\right) \tag{8}$$

where:

$$a^4 = \frac{\omega_j^2 \rho A}{EI}; \quad j = 1 \, to \, n \tag{9}$$

$$\alpha = \frac{\cos ax_c + \frac{\sin ax_c}{\tan a(L-x_c)}}{\cosh ax_c + \frac{\sinh ax_c}{\tanh a(L-x_c)}} \tag{10}$$

and the constant A_0 is chosen so that the mode shapes are normalized as:

$$\int_0^{x_c} \phi_j^2(\bar{x}) d\bar{x} + \int_{x_c}^{L} \phi_j^2(\bar{x}) d\bar{x} = 1 \tag{11}$$

The natural frequencies of the beam with the open crack can be calculated replacing boundary conditions in assumed solution of mode shape Eq (5):

$$\phi(x) = A_1 \cos ax + A_2 \sin ax + A_3 \cosh ax + A_4 \sinh ax \tag{12}$$

and setting its determinant to zero, or by using Eq. (9) and Eq. (10). A comparison of natural frequency results using the approach of Sundermeyer and Weaver (1994) was carried out against the approach of Narkis (1994) and the results were found to be in agreement. For a closed crack condition under compression, the natural frequency and the mode shape reduce to those obtained for a standard simply supported Euler Bernoulli beam and first mode shape is:

$$0 < x < L \quad \rightarrow \quad \phi(x) = \sqrt{\frac{2}{L}} \sin(ax) \tag{13}$$

Since the displacement at supports equals zero, the Eq. (12) is satisfied when *sin (aL) = 0*, therefore the natural frequencies of the beam when crack is closed are:

$$\omega_j = j^2 \pi^2 \sqrt{\frac{EI}{mL^4}}; \quad j = 1,2,3,... \tag{14}$$

The equation of motion of the vehicle, represented as a single degree of freedom oscillator can be represented as:

$$m_V \ddot{z} + K[z - r(t) - y(t,t)] = 0 \tag{15}$$

From ISO 8606:1995(E) specifications Road Surface Roughness (RSR) function in discrete form is:

$$r(\hat{x}) = \sum_{k=1}^{N} \sqrt{4S_d(f_0)\left(\frac{2\pi k}{L_c f_0}\right)^{-2} \frac{2\pi}{L_c}} \cos\left(\frac{2\pi k f_0}{L_c} + \theta_k\right) \tag{16}$$

The road classification according to ISO 8606:1995(E) is based on value of $S_d(f_0)$. Five classes of road surface roughness representing different qualities of the road surface are A (very good), B (good), C (average), D (poor), and E (very poor) with value of roughness coefficients 6×10^6, 16×10^6, 64×10^6, 256×10^6, and 1024×10^6 m^3/cycle, respectively. The bridge-vehicle interaction can finally be expressed as a system of two second order equations. For a first mode shape consideration (subscripted 1), Eq. (1) and Eq. (15) can be written in matrix form as:

$$\begin{bmatrix} 1 & 0 \\ 0 & 1 \end{bmatrix} \times \begin{Bmatrix} \ddot{q}_1 \\ \ddot{z} \end{Bmatrix} + \begin{bmatrix} 2\xi_1\omega_1 & 0 \\ 0 & 0 \end{bmatrix} \times \begin{Bmatrix} \dot{q}_1 \\ \dot{z} \end{Bmatrix} + \begin{bmatrix} \omega_1{}^2 + \frac{K}{\rho A}\phi_1(vt)\phi_1(vt) & \frac{K}{\rho A}\phi_1(vt) \\ -\omega_V{}^2 \phi_1(vt) & \omega_V{}^2 \end{bmatrix} \times \begin{Bmatrix} q_1 \\ z \end{Bmatrix} = \begin{Bmatrix} \frac{m_V g}{\rho A}\phi_1(vt) - \frac{K}{\rho A} r(vt)\phi_1(vt) \\ \omega_V{}^2 r(vt) \end{Bmatrix} \tag{17}$$

The displacements and velocities of the beam and the vehicle are obtained by using a 4/5th order Runge-Kutta method.

3 DAMAGE DETECTION USING SURFACE ROUGHNESS METHOD

The proposed concept of numerical analysis is shown in Figure. 2.

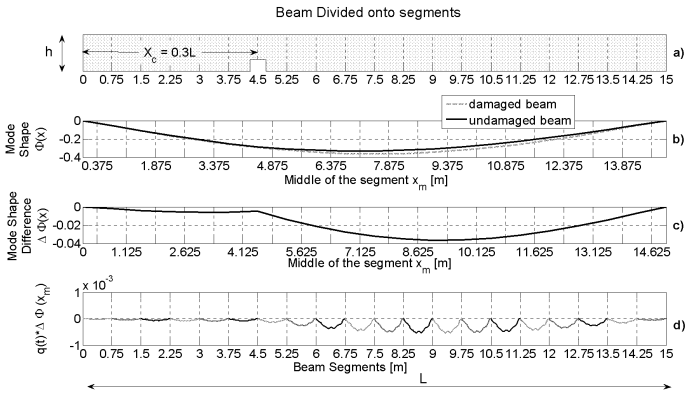

Figure 2. a) Simply supported beam with damage located at 0.3L (4.5m) divided into equal segments; b) Mode shape of damaged and undamaged beam; c) Difference in mode shape of undamaged and damaged beam (mode shape difference function); d) Mode shape difference function at mid location of each segment multiplied with temporal beam displacement.

The beam is divided into a number of equal segments, Fig. 2a. In this example the crack is located at x_c = 0.3L. Mode shapes for undamaged and damaged beam, shown in Fig. 2b, and $\Delta\Phi_m$ in Fig. 2c, are found. Function $\Delta\Phi_m$ has a local maximum and discontinuous slope at the damage location. The mode shape difference in the spatial domain in practice is hard to detect. For an experimental regime, an initial estimate of the undamaged mode shape and natural frequency should be carried out and the bridge response obtained is used to create a difference function in the time domain as $\Delta\Phi_m q(t)$, as shown in Fig. 2d. Noise is reduced by considering the passage of many vehicles and the consideration of normalisation. Figure 2 shows that the location near the damage is affected in this differenced time domain response. The data used for the bridge model are L = 15m, ξ = 2%, E = 200e9 N/m^2, and ρ = 7900 kg/m^3. The static deflection of the beam is 0.005 m based on this data. It is assumed that that the depth of the beam is 1.5 times the width of the beam. Other geometric descriptors like I, A and mass of the beam are computed based on this assumption. The data used for vehicle simulation are m_V = 3000 kg and K = 3.65e6 N/m.

4 MARKERS OF CALIBRATION

Statistical descriptors on previously determined functions ΔΦmq(t), for each segment of the observed beam are investigated for monotonocity and consistency. The statistical parameters of function ΔΦmq(t) considered included mean, standard deviation, skewness, and kurtosis. The choice of mean and standard deviation stemmed out of the recent study (Jaksic et al., 2011). The mean and standard deviation are computed as follows:

$$\mu = \frac{1}{m}\sum_{i=1}^{m} x_i \tag{1}$$

$$\sigma = \sqrt{\frac{1}{m}\sum_{i=1}^{m}(x_i - \mu)^2} \tag{1}$$

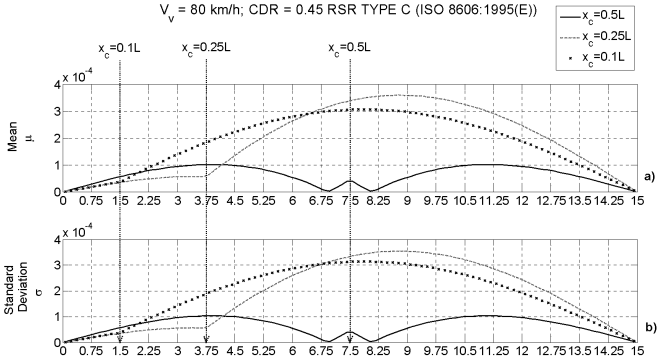

Figure 3. Static measures: a) Mean (μ) and b) Standard Deviation (σ). Figure shows statistics for crack located at 0.1L (1.5m), 0.25L (3.75m) from the left support and at mid-span 0.5L (7.5), Speed of the vehicle (V_V = 80km/h), Crack Depth Ratio (CDR = 0.45), and Type C Road Surface Roughness defined as per ISO 8606:1995(E).

Figure 3 shows an example of mean and standard deviation of $\Delta\Phi_m q(t)$ function calculated for each beam segment for the case of different position of the damage: edge, quarter-span and mid-span of the beam. The road type surface is class C, vehicle is moving with the constant speed 80km/h and CDR is 0.45 in this example. It is found that obtained mean and standard deviation functions are similar in shape and clearly show the discontinuous slope at the damage locations, similar to mode shape difference functions. This finding is consistent with the recent findings (Jaksic et al., 2011) where it has been proven that first and second order cumulants of bilinear and linear system response are consistent and monotonic descriptors of the system characteristics and are sensitive to system stiffness changes.

Values of μ and σ at crack locations for all combinations of x_c, RSR type, CDR, and Vv were investigated. More than 1800 cases were observed in order to establish the calibrations of μ and σ at crack loca-

tions and variable dependence / sensitivity of the calibrations.

From Fig. 3 and the similar figures obtained by varying x_C, CDR, RSR and Vv, a number of observations are noted. It is observed that the markers μ and σ show a derivative discontinuity at the damage location, values of statistical parameters relative to each other increase with decreasing road quality and μ and σ curves slope discontinuity at the crack location become more obvious for poor and very poor grades of road surface roughness. All of the above indicate that the location of crack can be identified by the chosen markers and that consistent calibration is possible.

5 RESULTS

Figure 4 represents an example of mean and standard deviation functions for the cases of different vehicle speed, ranging from 10km/h to 150km/h with 20km/h step moving on the average RSR (typeC).

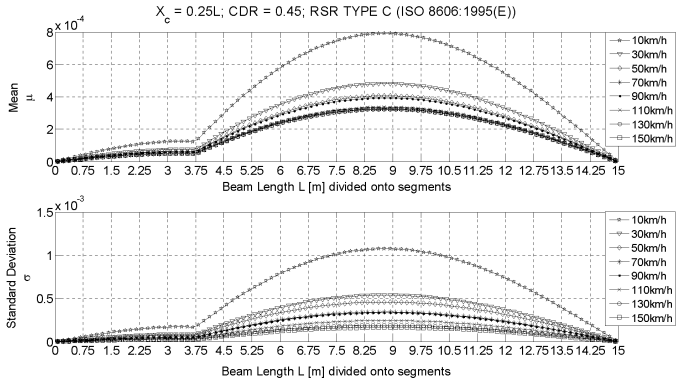

Figure 4. Mean (μ) and Standard Deviation (σ) for crack located at X_C = 0.25L (3.75m), Crack Depth Ratio CDR = 0.45, Type C Road Surface Roughness defined as per ISO 8606:1995(E), and different Vehicle Speed.

In this example the crack is located at quarter-span and CDR is 0.45 (large). It is observed that in general μ and σ values are higher for low vehicle speeds, in particular 10 km/h, and are decreasing with increasing vehicle speed. This is more evident in standard deviation figure (Fig. 4 bottom) while in the case of mean there is almost no difference for the vehicle speeds spanning 50 - 90 km/h or 110 - 150 km/h For thi particular example it is shown that the mean compared to standard deviation is less sensitive to increasing vehicle speed. The same conclusion was arrived t by observing different combinations of xc, CDR, and RSR. Therefore the sensitivity of the standard deviation marker was investigated and compared to the change of these variables.

For illustration purposes in Fig. 5 the standard deviation markers of CDR is presented for three different types of road, namely A, C and E, when the crack is located at mid span.

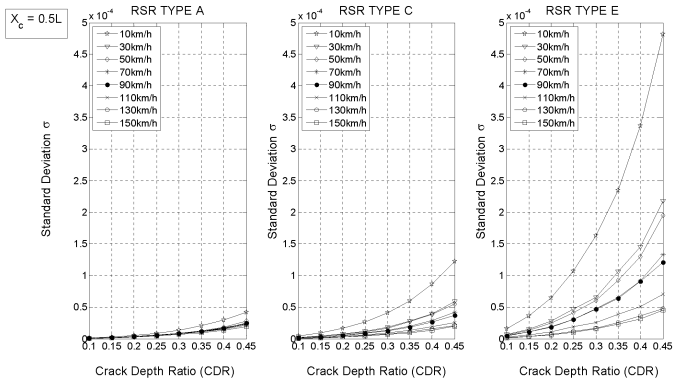

Figure 5. Standard Deviation (σ) variation in function of Crack Depth Ratio (CDR) for crack located at mid-span (7.5m), Type A (very good), C (average) and E (very poor) Road Surface Roughness defined as per ISO 8606:1995(E), and different Vehicle Speed.

It is observed that the relation between μ and σ and CDR for different V_V increases exponentially. It is noted that these curves are separated into 4 groups depending on V_V: very low speed 10km/h, low speed 20 to 60 km/h, medium speed 70 to 100km/h, and high speed 110 to 150km/h for which variation of μ and σ is very high, high, medium, and low, respectively. This grouping becomes more obvious for higher CDR when RSR is type D and E, while for the RSR type A and B there is very little difference between statistical parameters even for a higher values of CDR for medium and high speeds of the vehicle. The exception is very low V_V for which statistical parameters are observed to be much higher than for other V_V for all cases of RSR.

In order to determine which road surface is appropriate for calibration, standard deviation of the function of vehicle speed for crack located at mid-span with low, medium and high CDR is plotted in Fig. 6.

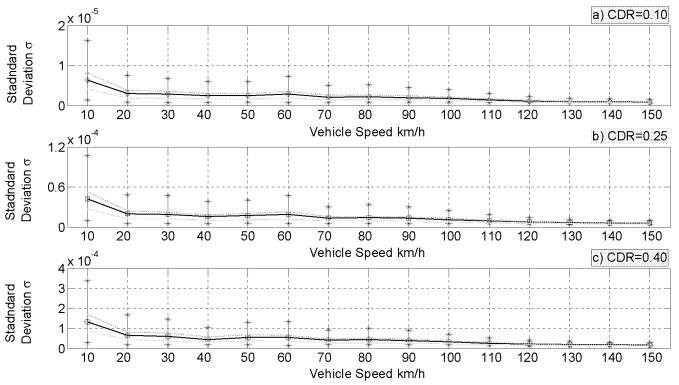

Figure 6. Variation of Standard Deviation (σ) in function of Vehicle Speed for crack located at mid-span (7.5m), Crack Depth Ratio a) low (0.1), b) medium (0.25) and c) high (0.4), Road Surface Roughness defined as per ISO 8606:1995(E).

The full lines in the figure indicate averaged value of standard deviation for all road types, while grey line bellow and dotted line above represent road type C and D respectively. The asterisks indicate extremes where low values represent road type A and higher values E. It is concluded that averaged values are very close to values obtained for road types class C and D (the curve is in between these two). Realistically, the average value is too high as standard deviation results for road type class E are way above results obtained for classes A, B and even C. Hence road type class C is found to be optimal for calibration purposes. In general, calibrations are monotonic (μ and σ increase with CDR) but there is no obvious relation between the curves representing different crack locations.

Figure 7 shows the results of calibration of standard deviation as a function of vehicle speed variation (low, medium, and high) observed for the position of damage close to the support (Fig. 7a), at quarter-span(Fig. 7b) and mid-span (Fig. 7c) of the beam. The calibration functions are shown for small (0.1), medium (0.25), and high (0.4) CDR. The dotted grey lines represents a 6th degree polynomial fit (which for the coefficients with 95% confidence bounds give the goodness of fit measure of R^2 as 0.9735 and 0.9865, for the worst and the best fit function respectively) which incorporates very low vehicle speeds. A speed of 10km/h shows much higher values of statistical descriptor when compared with other speeds. When the 10km/h value is excluded from the analysis, linear polynomial equations are obtained and represented with the solid line.

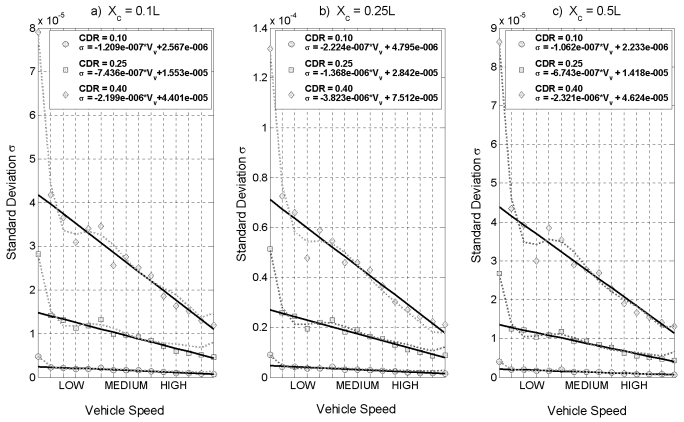

Figure 7: Calibration of Standard Deviation (STD) variation in function Vehicle Speed (Vv): Low, Medium and High; for three different position of damage: a) Edge, b) Quarter-span, and c) Mid-span.

6 CONCLUSIONS

The effect of vehicle speed for damage detection on bridges through consideration of bridge-vehicle interaction effects was studied. Mean and standard deviation of mode shape differenced temporal responses can be used as damage detection markers. Discontinuous slopes of mean and standard deviation curves give the position of damage while the jump size is related to the damage extent.

For the case when the road quality decreases the slope discontinuity of mean and standard deviation curves at the crack location become more obvious. This is amplified for poor and very poor grades of road surface roughness.

The consistency of calibration depends on vehicle speed and road surface type. This is more pronounced in the case of higher damage. The damage detection and calibration can be divided into low, medium and high speed zones.

The study is particularly useful for remote bridge health monitoring since the data necessary for analysis can be obtained from the operating condition of the bridge and the structure does not therefore need be closed down.

7 APPENDIX – DEFINITION OF SYMBOLS

A = cross-sectional area of the bridge (beam)
$A_{0\text{-}4}$ = mode shape function constants
a = variable dependant of the natural frequency of the bridge (beam)
CDR = Crack Depth Ratio
c = structural damping of the material of the bridge (beam)
E = Young's modulus of the material of the bridge (beam)
f_0 = the discontinuity frequency
g = acceleration due to gravity
I = second moment of area of the bridge (beam)
i = number of beams
j = number of mode shapes
K = equivalent stiffness of the vehicle's tires and springs
L = length of the bridge (beam)
L_c = twice the length of the bridge (beam)
m_V = mass of the vehicle
m = number of the beam segments
N = number of data points of successive ordinates of surface profile
P = external force
q_j = time dependent amplitude
RSR = Road Surface Roughness
$r(vt)$ = time domain sampling of road surface roughness
$S_d(f_0)$ = roughness coefficient
t = time coordinate with the origin at the instant of the force arriving upon the bridge (beam)

V_V = vehicle speed
x = length coordinate with the origin at the left-hand end of the bridge (beam)
$\bar{x}$ = spatial coordinate considered from left hand support
$\hat{x}$ = discrete representation of spatial coordinate
x_c = crack distance from the left support
$y_i(x,t)$ = transverse deflection of the i^{th} beam at the point x and time t, measured from the static equilibrium position due to self-weight
z = vertical displacement of the vehicle with respect to its static equilibrium position
α = variable dependant on natural frequency and clack location
δ = Dirac Delta function
θ_k = set of independent random phase angles uniformly distributed between 0 and 2π
μ = mean
ξ = damping ratio of the bridge (beam)
ρ = mass density of the bridge (beam) material
σ = standard deviation
υ = speed of the vehicle
ω_j = natural frequency of the bridge (beam)
ω_V = natural frequency of the vehicle
Φ_j^i = orthogonal mode shape of i^{th} beam for the j^{th} mode shape
$\Delta\Phi_m$ = difference between the damaged and undamaged mode shapes at the middle of the beam segments

8 ACKNOWLEDGEMENTS

The authors wish to thank the Irish Research Council for providing grant to support this research.

9 REFERENCES

Abdel-Rohman, M. & Al-Duaij, J., "Dynamic response of hinged-hinged single span bridges with uneven deck", Computers & Structures, Vol.59(2), pp.291-299, 1996.

Bilello, C. & Bergman, L. A., "Vibration of damaged beams under a moving mass: Theory and experimental validation", Journal of Sound and Vibration, Vol.274(3-5), pp.567–582, 2004.

Bu, J. Q., Law, S. S. & Zhu, X. Q., "Innovative bridge condition assessment from dynamic response of a passing vehicle", ASCE Journal of Engineering Mechanics, Vol.132(12), pp.1372–1379, 2006.

Cacciola, P., Impollonia, N. & Muscolino, G., "Crack detection and location in a damaged beam vibrating under white noise", Computers and Structures, Vol.81(pp.1773–1782, 2003.

Clough, R. W. & Penzien, J., *Dynamics of Structures*, second edition, McGraw-Hill Book Co., Singapore, 1993, 731.

da Silva, J. G. S., "Dynamical performance of highway bridge decks with irregular pavement surface", Computers & Structures, Vol.82(11-12), pp.871-881 2004.

Delgado, R. M. & dos Santos, R. C. S. M., "Modelling of a railway bridge–vehicle interaction on high speed tracks", Computers and Structures, Vol.63(3), pp.511-523 1997.

Farrar, C. R. & Worden, K., "An introduction to structural health monitoring", Philosofical Transactions of the Royal Society A: Mathematical, Phisical and Engineering Sciences, Vol.365(pp.303-315, 2007.

Friswell, M. I. & Penny, J. E. T., "Crack Modeling for Structural Health Monitoring", Structural Health Monitoring, Vol.1(2), pp.139 - 148, 2002.

Fryba, L., *Vibration of Solids and Structures under Moving Loads*, 3rd edition, Publishing house of Academy of Sciences of the Czech Republic, Thomas Telford Ltd., Prague, London, 1999,

Hadjileontiadis, L. J. & Douka, E., "Kurtosis analysis for crack detection in thin isotropic rectangular plates", Engineering Structures, Vol.29(9), pp.2353-2364, 2007.

Hadjileontiadis, L. J., Douka, E. & Trochidis, A., "Crack detection in beams using kurtosis", Computers & Structures, Vol.83(12–13), pp.909-919, 2005.

Harris, N. K., Gonzalez, A., Obrien, E. J. & McGetrick, P., "Characterisation of pavement profile heights using accelerometer readings and a combinatorial optimisation technique", Journal of Sound and Vibration, Vol.329(5), pp.497-508, 2010.

ISO 8606:1995(E). Mechanical vibration - road surface profiles-reporting of measured data.

Jaksic, V., Pakrashi, V. & O'Connor, A., "Employing Surface Roughness for Bridge-Vehicle Interaction based damage detection", *ASME 2011 International Mechanical Engineering Congress and Exposition (IMECE 2011)* Denver, Colorado, USA, 2011.

Kisa, M., "Free vibration analysis of a cantilever composite beam with multiple cracks", Composites Science and Technology, Vol.64(9), pp.1391–1402, 2004.

Law, S. S. & Zhu, X. Q., "Bridge dynamic responses due to road surface roughness and braking of vehicle", Journal of Sound and Vibration, Vol.282(3-5), pp.805-830 2005.

Law, S. S., Bub, J. Q., Zhua, X. Q. & Chana, S. L., "Vehicle axle loads identification using finite element method", Engineering Structures, Vol.26(8), pp.1143-1153 2004.

Loutridis, S., Doukab, E. & Trochidis, A., "Crack identification in double-cracked beams using wavelet analysis ", Journal of Sound and Vibration, Vol.277(4-5), pp.1025-1039 2004.

Majumder, L. & Manohar, C. S., "A time domain approach for damage detection in beam structures using vibration data with a moving oscillator as an excitation source. ", Journal of Sound and Vibration, Vol.268(pp. 699–716, 2003.

MATLAB 7, The MathWorks, Inc., Natick, MA, 2004.

Moyo, P. & Brownjohn, J. M. W., "Detection of Anomalous Structural Behaviours using Wavelet Analysis", Mechanical Systems and Signal Processing Vol.16(2-3), pp.429-445, 2002.

Narkis, Y., "Identification of crack Location in vibrating simply supported beams", Journal of sound and Vibrations, Vol.172(4), pp.Pages 549-558 1994.

O'Brien, E., Li , Y. & Gonzalez, A., "Bridge roughness index as an indicator of bridge dynamic amplification", Compurers & Structures, Vol.Volume 84(12), pp.759–769, 2006.

Okafor, A. C. & Dutta, A., "Structural damage detection in beams by wavelet transforms", Smart Materials and Structures, Vol.9(6), pp.906–917, 2000.

Pakrashi, V., Basu, B. & Connor, A. O., "A Statistical Measure for Wavelet Based Singularity Detection", Journal of Vibration and Acoustics, Vol.131(4), pp.041015 (6 pages) 2009.

Pakrashi, V., O'Connor, A. & Basu, B., "A Bridge–Vehicle Interaction Based Experimental Investigation of Damage Evolution", Structural Health Monitoring, Vol.9(4), pp.285 - 296, 2010.

Pesterev, A. V. & Bergman, L. A., “Vibration of elastic continuum carrying accelerating oscillator”, ASCE Journal of Engineering Mechanics, Vol.123(8), pp.886-889, 1997.
Poudel, U. P., Fu, G. & Ye, J., “Structural damage detection using digital video imaging technique and wavelet transformation”, Journal of Sound and Vibration, Vol.286(4-5), pp.869–895, 2005.
Rucka, M. & Wilde, K., “Crack identification using wavelets on experimental static deflection profiles”, Engineering Structures, Vol.28(2), pp.279–288, 2006.
Sohn, H., Farrar, C. R., Hunter, N. F. & Worden, K., “Structural Health Monitoring using Statistical Pattern Recognition Techniques”, ASME Journal of Dynamic Systems, Measurement and Control Vol.123(4), pp.706-717, 2001.
Sundermeyer, J. N. & Weaver, R. L., “On Crack Identification and Characterization in a beam by non-linear vibration analysis”, Journal of Sound and Vibration, Vol.183(5), pp.857-871, 1994.